

## Supplementary Material

### Plasmon-coupled Au-nanochain functionalized PEDOT:PSS for efficient mixed tin-lead iodide perovskite solar cell

Jiaxing Song<sup>a</sup>, Xinxing Yin<sup>a</sup>, Lin Hu<sup>a</sup>, Zhen Su<sup>a</sup>, Yingzhi Jin<sup>a</sup>, Dan Deng<sup>a</sup>, Zaifang Li<sup>a\*</sup>, Guannan Wang<sup>b\*</sup>, Qinye Bao<sup>d</sup> and Wenjing Tian<sup>c\*</sup>

<sup>a</sup> China-Australia Institute for Advanced Materials and Manufacturing, Jiaxing University, Jiaxing 314001, PR China

<sup>b</sup> College of Biomedical Engineering & the Key Laboratory for Medical Functional Nanomaterials, Jining Medical University, Jining 272067, PR China

<sup>c</sup> State Key Laboratory of Supramolecular Structure and Materials, Jilin University, Changchun 130012, PR China

<sup>d</sup> Key Laboratory of Polar Materials and Devices, School of Physics and Electronic Science, East China Normal University, Shanghai 200241, PR China

## Experimental

### Materials

Poly(3,4-ethylenedioxythiophene):poly-(styrene sulfonate) (PEDOT:PSS) (Clevious P VP AI 4083, 1.3~1.7 wt% dispersion in H<sub>2</sub>O), PbI<sub>2</sub> (>99.99%), CH<sub>3</sub>NH<sub>3</sub>I (MAI, ≥99.5%), HC(NH<sub>2</sub>)<sub>2</sub>I (FAI, ≥99.5%), C<sub>60</sub> (99.9%), and BCP (99.9%) were purchased from Xi'an Polymer Light Technology Co. (PLT). The SnI<sub>2</sub> (beads, -10 mesh, 99.99% trace metals basis), formamidinium sulfonic acid (FSA, ≥98%) and tin powders (99.5%) were purchased from Sigma-Aldrich. SnF<sub>2</sub> (99%) was obtained from Acros. Ultradry solvent of N, N-dimethyl formamide (DMF, >99.9%) and Dimethyl sulfoxide (DMSO, >99.9%) were

obtained from J&K. All the chemicals and solvents were kept in the glove-box before starting our experiment.

### **Synthesis of AuNCs**

Firstly, the Au nanoparticles (AuNPs) were synthesized following Frens' method.[1] In general, under thoroughly stirring, 1.0 mL 12 mg/mL H<sub>2</sub>AuCl<sub>4</sub> was added into 79 mL H<sub>2</sub>O at 90 °C. The reductant mixtures, composed with 4.0 mL 10 mg/mL tri-sodium citrate, 1.0 mL 25 mM Na<sub>2</sub>CO<sub>3</sub>, and 15 mL H<sub>2</sub>O were also heated to 90 °C. The reductant mixtures were poured into the H<sub>2</sub>AuCl<sub>4</sub> solution and the reaction was kept at 90 °C for 10 min. After that, the solution was gradually cooled down to room temperature within 3 h and the stirring was kept. Some deionized water was replenished to get about 100 mL colloid solution in the end. Then, 5 μL HS-C<sub>2</sub>H<sub>4</sub>-COOH was added into the solution with slightly shaking overnight. The resulting solution was stored at 4 °C. Then the 9.09×10<sup>-7</sup> M melamine stock solution was individually injected with stirring to get for aggregated AuNPs to form the Au nanochains (AuNCs). The concentration of AuNCs is about 2 mg/ml.

### **Perovskite precursor solution**

The precursor solution (1.8 M) was prepared by mixing solvents of DMF and DMSO with a volume ratio of 3: 1. The molar ratios for FAI/MAI and PbI<sub>2</sub>/SnI<sub>2</sub> were 0.7: 0.3 and 0.5: 0.5, respectively. The molar ratio of (FAI+MAI)/(PbI<sub>2</sub>+SnI<sub>2</sub>) was 1: 1. SnF<sub>2</sub> (10 mol% relative to SnI<sub>2</sub>), FSA(0.3 mol%), and tin powders (5 mg ml<sup>-1</sup>) were added in the precursor solution. The precursor solution was stirred at room temperature for 1 h, and that was filtered through a 0.22 μm polytetrafluoroethylene (PTFE) membrane before preparing the perovskite films.

### **Device fabrication**

The pre-patterned ITO substrates were cleaned with detergent, deionized water, acetone, and 2-propanol in sequence. The AuNCs aqueous solution with a certain amount (0, 0.5, 1 or 2 wt%) was added into PEDOT:PSS, and the solution was kept stirring for 1h. Then, the blended PEDOT:PSS-AuNCs solution was spin-coated on ITO substrates at 4000 rpm

for 50 s and the films were annealed at 150 °C for 10 min in ambient air. After that, the FA<sub>0.7</sub>MA<sub>0.3</sub>Sn<sub>0.5</sub>Pb<sub>0.5</sub>I<sub>3</sub> precursors were spin-coated onto PEDOT:PSS with a two-step spin-coating procedure: 1000 rpm for 10 s and 4000 rpm for 40 s. Diethyl ether was dropped on the spinning substrate during the second spin-coating step at 20 s before the end. The substrates were then transferred onto a hotplate and heated at 100 °C for 10 min in a glove box. Finally, C<sub>60</sub>(20 nm)/BCP(5 nm)/Cu (80 nm) were sequentially deposited by thermal evaporation through a shadow mask with an active area of 0.0945 cm<sup>2</sup>.

### 2.3 Device characterization

The current density-voltage ( $J$ - $V$ ) characteristics of solar cells were measured in glove-box under 100 mW/cm<sup>2</sup> AM 1.5G solar irradiation (Enlitech SS-F5-3A) with a Keithley 2400 Source Meter, and the irradiation intensity was calibrated by a monocrystalline silicon reference cell (Enlitech SRC-00207). Generally, the devices were directly placed under 100 mW/cm<sup>2</sup> illumination, and then the  $J$ - $V$  measurement was performed at the scan rate of 120 mV/s without pre-bias. The EQE was measured by Solar Cell Spectral Response Measurement System (Enlitech QE-R3018). The light intensity at each wavelength was calibrated with a standard single-crystal Si photovoltaic cell. The IQE was calculated by normalizing the EQE spectrum of the device by the absorption spectrum (IQE=EQE/A). For transient photocurrent measurement, the system is similar to that reported previously.[2] The durability of devices were explored by performing the  $J$ - $V$  characterization periodically under 100 mW/cm<sup>2</sup> AM 1.5G solar irradiation in glove-box, and the unencapsulated devices were stored in glove-box in the rest time. As for SCLC measurements, the mobility values were calculated by fitting the dark  $J$ - $V$  curves of hole-only devices according to the following equation:  $J=9/8\epsilon_0\epsilon_r\mu_0(V-V_{bi})^2/L^3\exp(0.89\beta(V-V_{bi})^{0.5}/L^{0.5})$ , and the device structure is ITO/HTL/FA<sub>0.7</sub>MA<sub>0.3</sub>Sn<sub>0.5</sub>Pb<sub>0.5</sub>I<sub>3</sub>/MoO<sub>3</sub>/Ag. The dependence of  $J_{sc}$  on  $P_{light}$  can provide information on the bimolecular recombination occurring in the photoactive layer, which follows a power law dependence, that is,  $J_{sc} \propto P_{light}^\alpha$ . The power-law exponent  $\alpha$  will equal to unity when all carriers are swept out prior to recombination, deviation from  $\alpha=1$  is conjectured to arise from a small loss of carriers via bimolecular recombination. The  $V_{oc}$  varies logarithmically with  $P_{light}$  and follows the relationships of  $V_{oc} \propto (nkT/q)\ln(P_{light})$ . Under open-circuit conditions, all

photogenerated free carriers recombine, and the slope of  $V_{oc}$  versus logarithmical  $P_{light}$  will be equal to  $kT/q$  if bimolecular recombination dominates, while the deviated slope from  $kT/q$  suggests that additional trap-assisted Shockley–Read–Hall (SRH) recombination is involved.

## 2.4 Thin film characterization

Film thicknesses were measured using a Veeco Dektak XT surface profilometer. UV-Vis-NIR and normal incident reflection spectra were obtained using a Shimadzu 3600 spectrophotometer. A field emission scanning electron microscope (Hitachi SU8010, Hitachi S-4800) was used to acquire SEM images. ASPM-9700 from Shimadzu was used to acquire AFM images. Transmission electron microscopy (TEM) was conducted using a Hitachi H-800 electron microscope at an acceleration voltage of 200 kV with a CCD camera. For steady-state PL, a 532 nm cw laser beam at  $110 \text{ mW cm}^{-2}$  was used as a source of excitation. The PL signal was detected by a Horiba Symphony-IICCD detector. UPS and XPS were performed in an ultrahigh vacuum surface analysis system equipped with a fast entry load-lock, a transfer chamber, and an analysis chamber (base pressure  $\approx 10^{-10}$  mbar). UPS employed the HeI (21.22 eV) as the excitation source with an energy resolution of 50 meV. XPS was measured using the monochromatic Al K $\alpha$  (1486.6 eV).

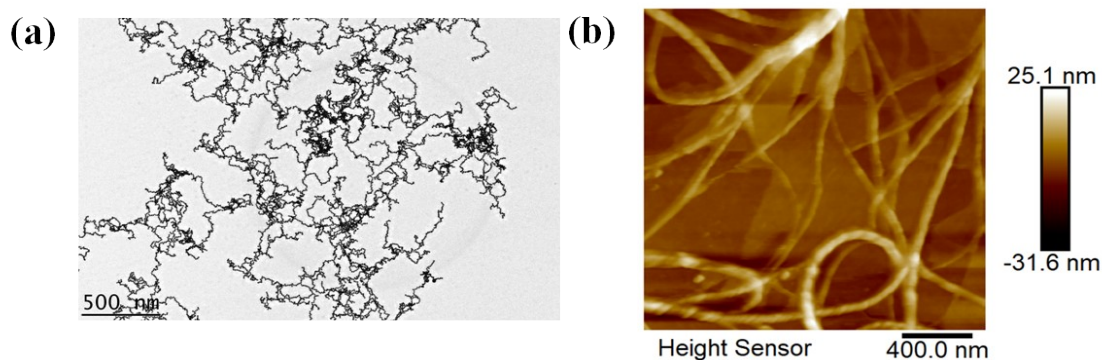


**Figure S1.** (a) The TEM images of AuNCs with low magnification, the scale bar is 500 nm. (b) The AFM image of AuNCs.

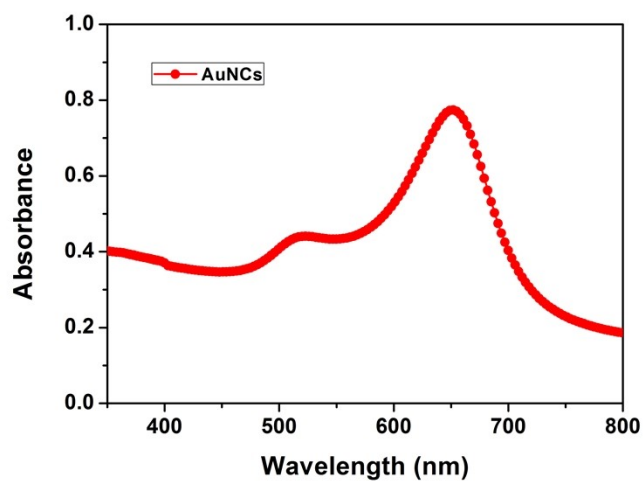


**Figure S2.** The absorption spectrum of as-prepared AuNCs.

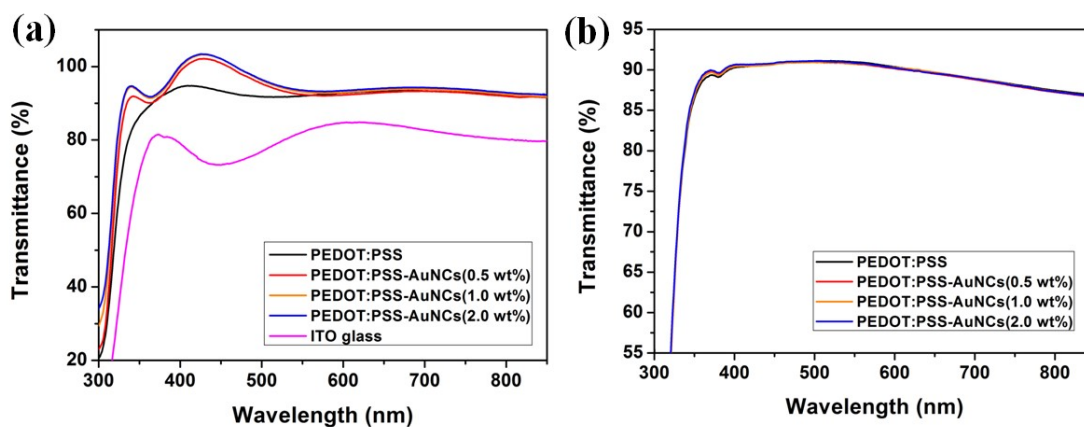


**Figure S3.** The transmission spectra of PEDOT:PSS HTLs with varied AuNCs on the (a) ITO glass and (b) quartz substrates, respectively. Bare ITO glass is included as the control.

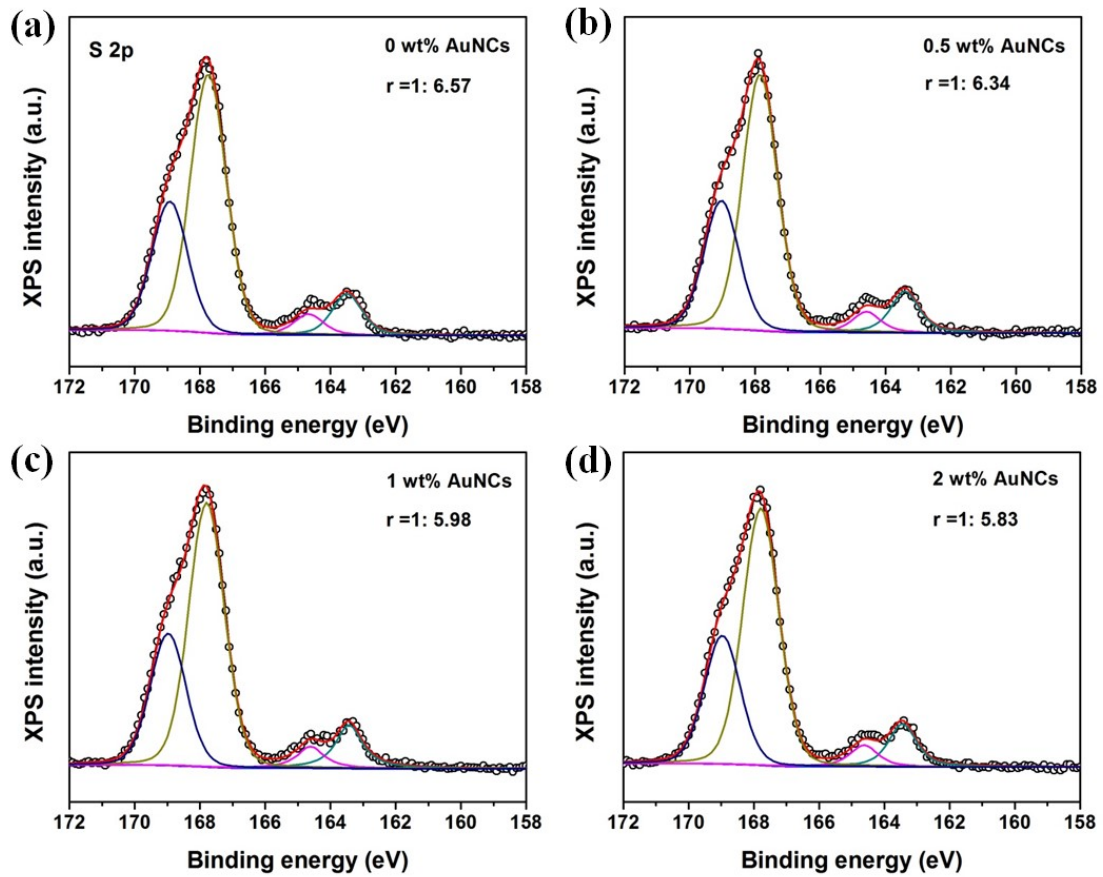


**Figure S4.** The XPS spectra of S 2p for PEDOT:PSS films with different content of AuNCs.

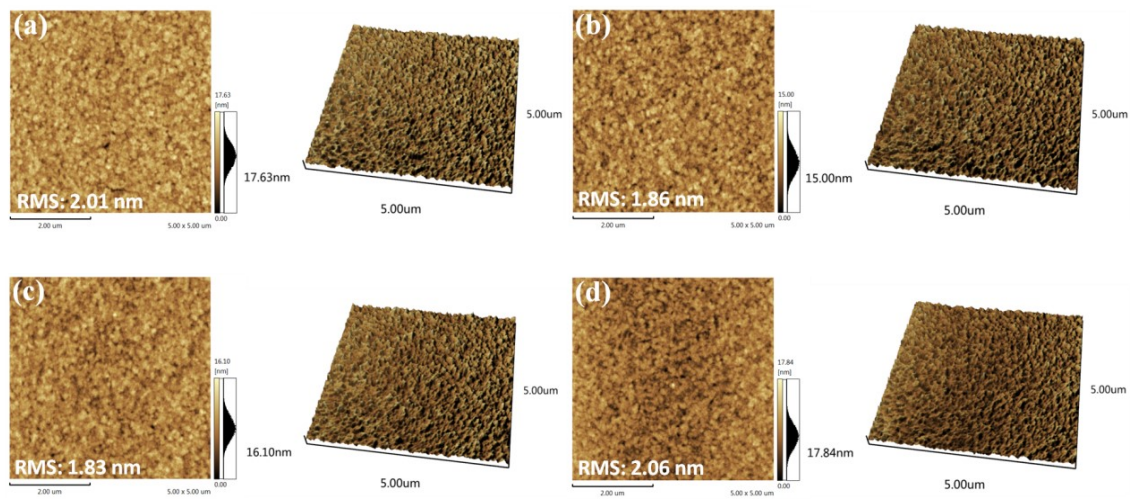


**Figure S5.** AFM topography images of (a) pristine PEDOT:PSS, and (b-d) PEDOT:PSS films with 0.5 wt%, 1.0 wt%, and 2.0 wt% AuNCs, respectively. The area is  $5.0 \times 5.0 \mu\text{m}^2$ .

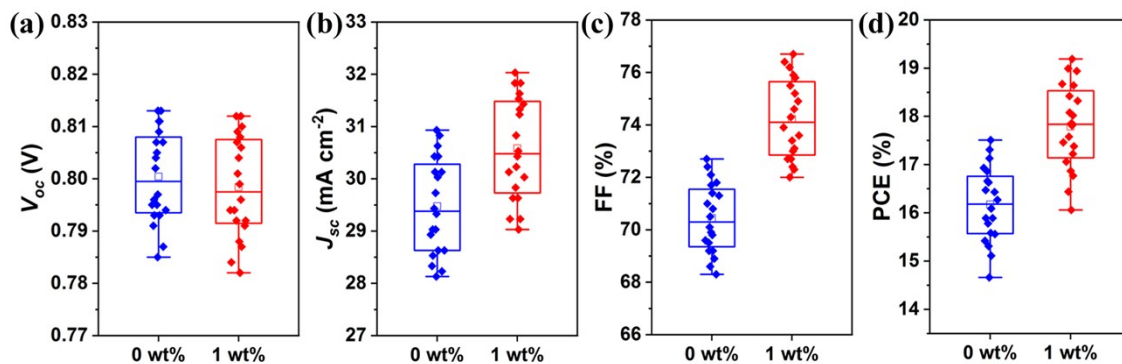


**Figure S6.** Statistical photovoltaic parameters obtained from 20 PSCs based on the HTLs without and with optimal 1 wt% AuNCs, (a)  $V_{oc}$ , (b)  $J_{sc}$ , (c) FF, (d) PCE.

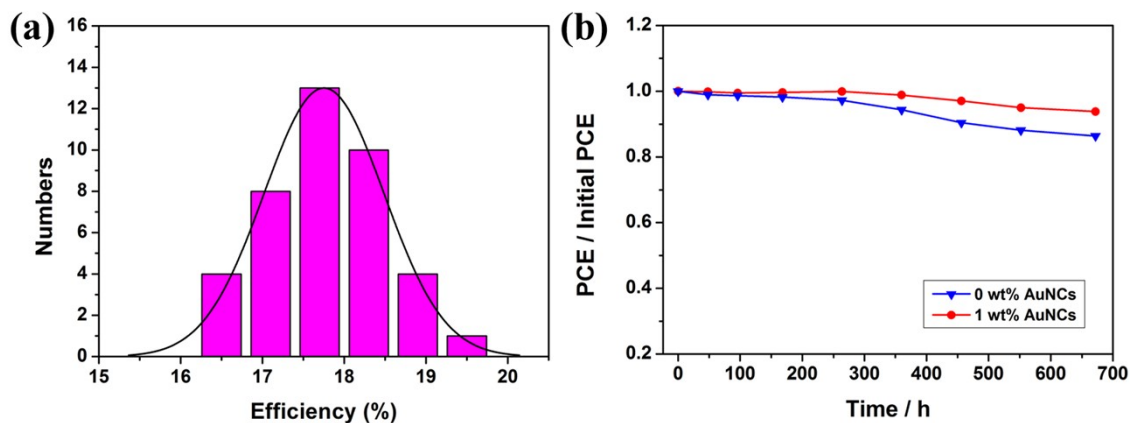


**Figure S7.** (a) Histograms of PCEs measured for 40 PSCs with optimal 1 wt% AuNCs. (b) Durability of the unencapsulated devices without and with AuNCs stored in a glove-box.

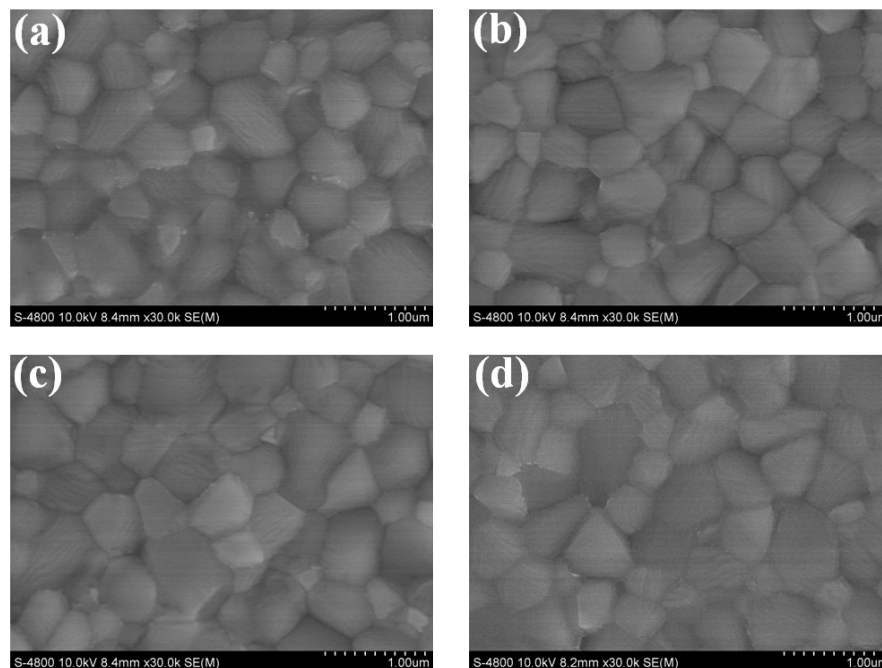


**Figure S8.** Top-view SEM images of perovskite film on different HTLs: (a) PEDOT:PSS, (b) PEDOT:PSS-AuNCs (0.5 wt%), (c) PEDOT:PSS-AuNCs (1.0 wt%) and (d) PEDOT:PSS-AuNCs (2.0 wt%). The scale bar is 1  $\mu\text{m}$ .

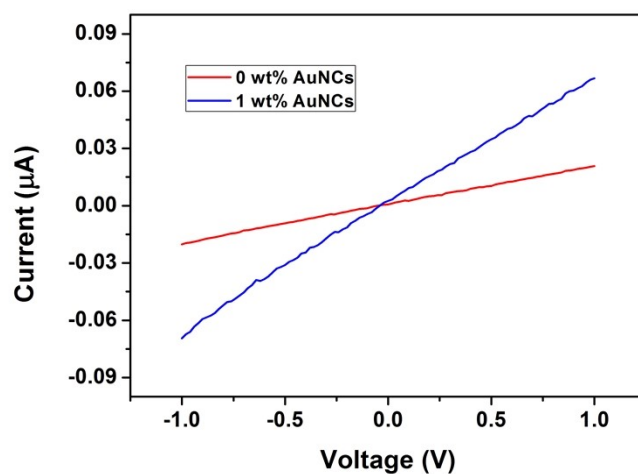


**Figure S9.** The current-voltage (I-V) characteristics of the PEDOT:PSS films. The conductivity ( $\sigma$ ) is proportional to the current and determined by  $\sigma=L/(R \cdot A)=I \cdot L/(U \cdot A)$ . L

is the distance between the two electrodes, R is the resistance and A is the cross-sectional area of films.

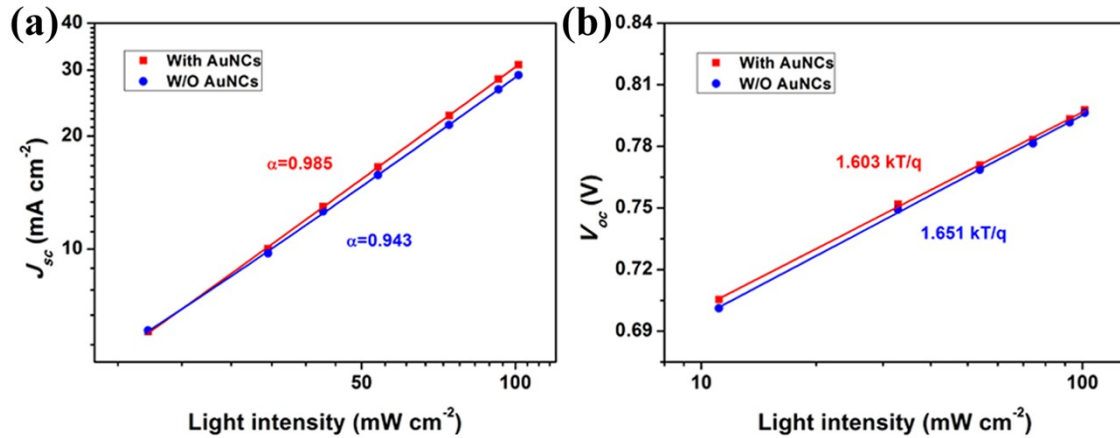


**Figure S10.** (a)  $J_{sc}$  and (b)  $V_{oc}$  as function of light intensity for PSCs with and without AuNCs.

### The effect of AuNCs on the band structure of HTLs

The ultraviolet photoelectron spectroscopy (UPS) of these PEDOT:PSS films was also characterized. As shown in **Fig. S9**, the work function ( $W_F$ ) of HTLs is slightly elevated from -4.97 eV to -4.86 eV as the content of AuNCs increases, determined by the difference between the photon energy (21.22 eV) and the value of  $E_{cutoff}$ . It is reported that the  $V_{oc}$  is proportional to the quasi-Fermi level difference between ETL and HTL.[3] In this case, the  $W_F$  result is consistent with the decreasing trend of  $V_{oc}$  listed in **Table 1**. Nevertheless, the addition of AuNCs affected the variation of  $V_{oc}$  values of PSC devices minimally, especially when the content of AuNCs is no more than the optimal 1 wt%. The reduced recombination energy loss derived from improved interfacial trap-state might somewhat mitigate the effect of band structure on  $V_{oc}$ .

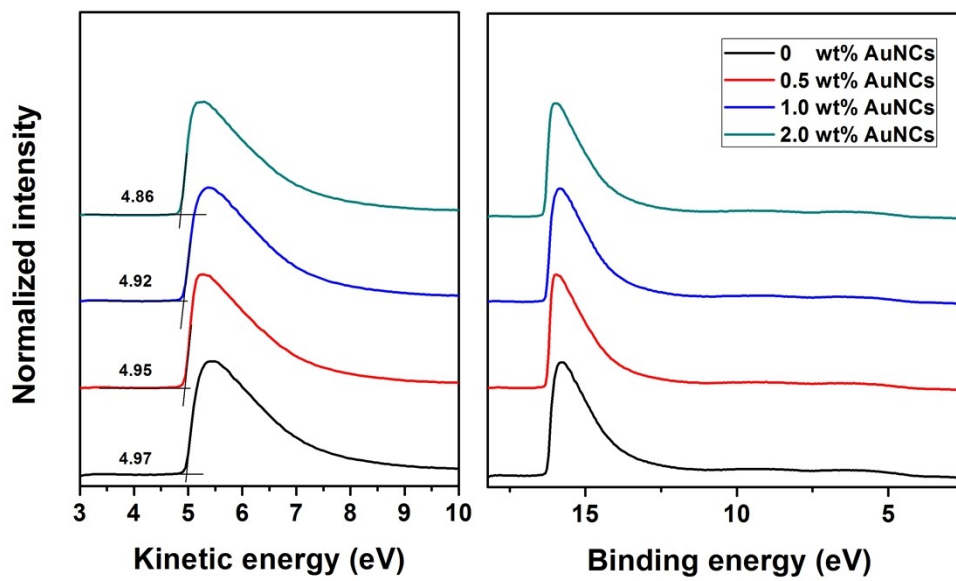


**Figure S11.** UPS spectra of PEDOT:PSS HTLs with various content of AuNCs: work function (left) and cutoff region (right).

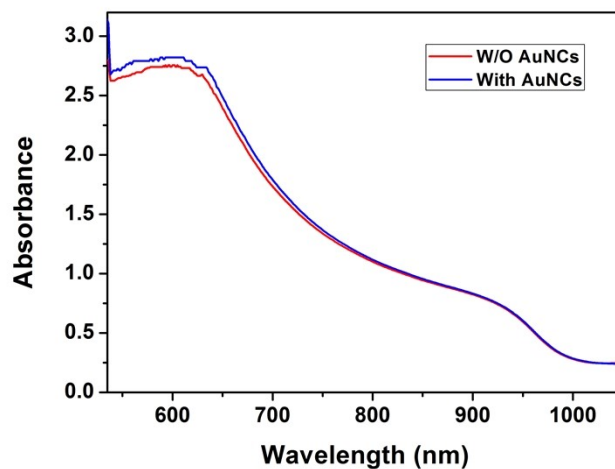


**Figure S12.** UV-vis absorption spectrum of perovskite films based on PEDOT:PSS HTL without and with AuNCs (1 wt%).

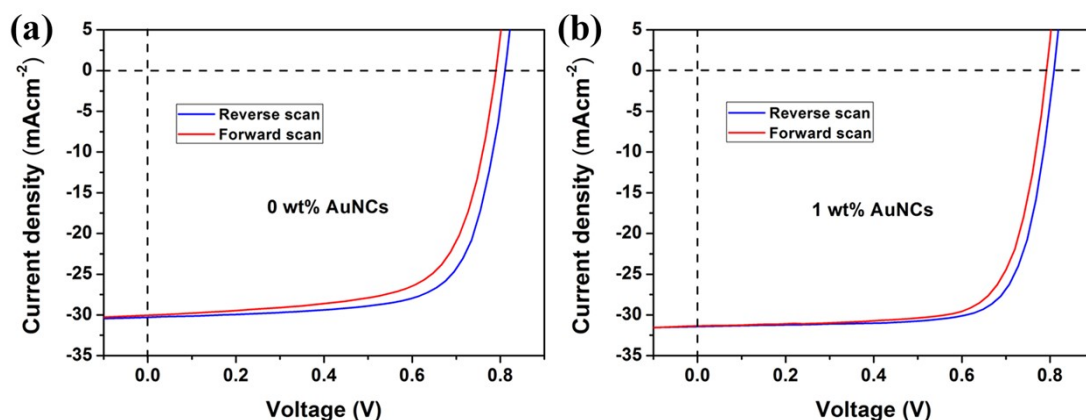


**Figure S13.** The  $J$ - $V$  characteristics of devices a) without and b) with 1 wt% AuNCs measured at  $100 \text{ mWcm}^{-2}$  AM 1.5G illumination under different scanning directions.

**Table S1.** The corresponding photovoltaic performance parameters for PSC devices under different scanning directions in Figure S13.

AuNCs concentration	Direction	$V_{oc}$ / V	$J_{sc}$ / $\text{mA cm}^{-2}$	FF / %	PCE / %
0 wt%	forward	0.790	30.05	67.8	16.10
	reverse	0.811	30.28	71.3	17.51
1 wt%	forward	0.792	31.35	73.5	18.25
	reverse	0.809	31.43	75.5	19.20

## References

- [1] G. Frens, Controlled nucleation for the regulation of the particle size in monodisperse gold suspensions. *Nature Phys. Sci.*, 1973, **241**(105), 20-22.
- [2] Y. Li, Y. Zhao, Q. Chen, Y. (Michael) Yang, Y. Liu, Z. Hong, Z. Liu, Y.-T. Hsieh, L. Meng, Y. Li, Y. Yang, Multifunctional fullerene derivative for interface engineering in perovskite solar cells, *J. Am. Chem. Soc.* 2015, **137**, 15540-15547.
- [3] H. Kim, K.-G. Lim, T.-W. Lee, Planar heterojunction organometal halide perovskite solar cells: roles of interfacial layers, *Energy Environ. Sci.* 2016, **9**, 12-30.